DESIGN, DEVELOPMENT, AND CHARACTERIZATION OF *SOLANUM XANTHOCARPUM* NANO-SUSPENSION: IN VITRO EVALUATION AND HEPATOPROTECTIVE STUDY IN VPA-INDUCED RATS

K. Sridevi
Dept of Pharmacy
Glocal University
Uttar Pradesh.

Dr. Jayesh Dwivedi
Dept of Pharmacy
Glocal University
Uttar Pradesh.

Abstract: *The study aims to assess the hepatoprotective impact of methanolic stem extract from Solanum xanthocarpum in rats that have been treated with VPA. The extract was made using Soxhlet's apparatus, and PVA stabilizer was used to create a nanosuspension utilizing a precipitation method. Extract and Nanosuspension formulation had characterize by different analytical methods like Fourier transform infrared spectroscopy, Scanning electron microscopy, Zeta potential and Particle size distribution, Differential scanning calorimeter and XRD. Hepatoprotective effects have been studied by performing in-vitro and in-vivo. In vitro Human hepatoblastoma cells line activity. IC50 determination, MTT cell proliferation assay, Microscopy observations and Statistical analysis. Animal study in five groups, Normal, Induced by VPA (500 mg/kg), VPA+STD- silymarin group: (500 mg/kg + 100 mg/kg p.o), VPA+ Extract group: (500 mg/kg + 300 mg/kg) and VPA+ Nanosuspension group: (500 mg/kg + Nanosuspension). After animal study examine like liver weight, biochemical analysis, oxidative stress, inflammatory cytokines and histopathology.*

Introduction:

Hepatoprotection refers to the capacity of a substance to prevent damage to the liver, a vital organ responsible for metabolic, detoxifying, and synthetic functions in the body. Liver diseases, including hepatitis, cirrhosis, and non-alcoholic fatty liver disease (NAFLD), are major global health problems that contribute significantly to morbidity and mortality (Salar et al., 2023). Hepatoprotective agents, both synthetic and natural, play a crucial role in mitigating liver injury caused by infections, toxic substances, and metabolic stress. Over recent years, a growing body of research has focused on natural hepatoprotective agents, particularly plant-based extracts, due to their favorable safety profiles and potential therapeutic efficacy (Ahmad et al., 2023; Arman et al., 2022; Ayenew and Wasihun, 2023).

The epidemiology, liver diseases are prevalent globally, with significant variations in incidence and mortality across different regions. Worldwide, approximately 2 million people die from liver disease each year, with about half of these deaths attributed to cirrhosis and the other half to viral hepatitis and hepatocellular carcinoma (Kim, 2022; Kulik and El-Serag, 2019). Hepatitis B and C viruses are the major contributors to chronic liver disease globally, especially in regions like sub-Saharan Africa and East Asia. In Western countries, alcohol-related liver disease and NAFLD are leading causes of liver dysfunction. NAFLD, associated with obesity and metabolic syndrome, is becoming increasingly prevalent, affecting approximately 25% of the global population (Singal et al., 2023; Xiao et al., 2023). In

India, liver diseases are also a major public health concern. The prevalence of NAFLD in the Indian population is around 9% to 32%, with significant associations with obesity, diabetes, and metabolic syndrome. Chronic hepatitis infections are also a serious issue, particularly hepatitis B, which affects around 40 million people in India, making it a major endemic region for the virus (Vaz et al., 2023). The increasing burden of liver disease in India can be linked to rising lifestyle-related conditions, such as diabetes and obesity, as well as the continued prevalence of infectious hepatitis (Haqqi et al., 2019).

The modern therapeutic approaches to liver disease focus on herbal medicine also extends to the development of advanced formulations, such as standardized extracts and nanotechnology-based delivery systems (Jain et al., 2020; Kumar et al., 2020). Standardization ensures that the active compounds in herbal extracts are present at consistent, therapeutic levels, which improves efficacy and safety. Nanotechnology, as mentioned earlier with nanosuspensions, enhances the bioavailability and targeted delivery of herbal compounds, offering a significant improvement over traditional herbal formulations (Harakeh et al., 2023). One of the most compelling examples of modern herbal therapeutics is the use of *Solanum xanthocarpum* extract in the form of nanosuspensions for hepatoprotection. This formulation capitalizes on the plant's potent bioactive compounds, which have been shown to reduce liver inflammation, oxidative stress, and fat accumulation (Kumar and Pandey, 2022; Sahu et al., 2024). By incorporating nanosuspension technology, these extracts achieve improved absorption, stability, and therapeutic outcomes, making them a promising alternative for the treatment of liver diseases such as NAFLD, hepatitis, and liver fibrosis. The integration of herbal medicine into modern therapeutic approaches for liver diseases reflects a growing recognition of the benefits of natural compounds (Kumar et al., 2023). Herbal remedies, enhanced by modern technologies like nanotechnology, offer safer, more holistic, and potentially more effective treatments for liver disorders (Hussain et al., 2012).

Natural hepatoprotective agent gaining significant attention is *Solanum xanthocarpum*, a plant widely used in traditional Indian medicine (Ayurveda) for its medicinal properties. Extracts from this plant have demonstrated a range of pharmacological activities, including anti-inflammatory, antioxidant, antidiabetic, and hepatoprotective effects (Konar and Chatterjee, 2022). The hepatoprotective potential of Solanum xanthocarpum is mainly attributed to its rich content of bioactive compounds like alkaloids, flavonoids, glycosides, and saponins, which have shown promise in protecting liver cells from damage caused by toxins, alcohol, and oxidative stress. These compounds can help restore the liver's natural antioxidant defense system, inhibit lipid peroxidation, and prevent the depletion of endogenous antioxidants such as glutathione (Nithya et al., 2018; Thapa et al., 2022; Xu et al., 2022). *Solanum xanthocarpum* is driven by a desire to minimize the side effects and long-term risks

associated with conventional treatments. Unlike synthetic drugs, which often target specific pathways, natural compounds typically exert their effects through multiple mechanisms, providing a holistic approach to disease management. Moreover, plant-based therapies are generally better tolerated, even with prolonged use, and tend to have fewer adverse effects (Mahalakshmi et al., 2019). This makes them particularly attractive for the treatment of chronic conditions like liver diseases, where long-term management is essential. In recent years, the advent of nanotechnology has opened new avenues for enhancing the efficacy and bioavailability of natural compounds, including those derived from *Solanum xanthocarpum*. Nanosuspensions of *Solanum xanthocarpum* extracts represent a promising development in this field (Liu et al., 2024). Nanosuspension refers to a colloidal dispersion of submicron-sized drug particles, which can improve the solubility, stability, and bioavailability of poorly soluble compounds. When herbal extracts are converted into nanosuspensions, their therapeutic efficacy can be significantly enhanced, allowing for better penetration into target tissues and cells, including liver cells (Kumar and Pandey, 2014).

Solanum xanthocarpum nanosuspensions offer several advantages over traditional extracts. First, the smaller particle size in nanosuspensions allows for a larger surface area, which enhances the dissolution rate of the active compounds. This results in improved absorption and higher bioavailability when administered orally or through other routes (Li et al., 2021). Second, the nanosuspension formulation can protect the bioactive compounds from degradation in the gastrointestinal tract, ensuring that a higher proportion of the active ingredients reach the liver. This is particularly important for plant-based compounds, which are often susceptible to degradation by enzymes and acidic conditions in the stomach. Third, nanosuspensions can provide controlled and sustained release of the bioactive compounds, maintaining therapeutic levels in the bloodstream for longer periods and reducing the need for frequent dosing. This is particularly beneficial in chronic liver diseases, where long-term treatment is required (Ma et al., 2023).

The significance of *Solanum xanthocarpum* nanosuspensions in the treatment of liver diseases lies in their ability to target multiple pathways involved in liver damage (Gautam et al., 2023). The bioactive compounds in the plant extracts can scavenge free radicals, inhibit inflammatory cytokines, and modulate metabolic pathways to reduce fat accumulation in the liver. Moreover, nanosuspensions can enhance the delivery of these compounds to the liver, ensuring that they reach the site of damage and exert their protective effects more effectively. This is particularly relevant in conditions like NAFLD, where oxidative stress and inflammation play key roles in disease progression. By reducing oxidative stress and inflammation, *Solanum xanthocarpum* extracts can help prevent the progression of NAFLD to more severe forms of liver disease, such as cirrhosis and hepatocellular carcinoma (Coronati et al., 2022). Liver diseases continue to pose a significant global

health challenge, with millions of people affected worldwide. While modern therapeutic agents have provided effective treatments for conditions like viral hepatitis, the long-term risks and side effects associated with these drugs have led to a growing interest in natural alternatives. *Solanum xanthocarpum* extracts have shown considerable potential as hepatoprotective agents due to their antioxidant, anti-inflammatory, and hepatoprotective properties (Pervez et al., 2023). The development of nanosuspensions of *Solanum xanthocarpum* extracts represents a promising step forward, as this technology enhances the bioavailability and therapeutic efficacy of the plant's bioactive compounds. By leveraging the benefits of nanotechnology, these formulations could offer a safer, more effective approach to managing liver diseases, particularly in chronic conditions where long-term treatment is essential. This shift towards natural compounds, particularly in advanced formulations like nanosuspensions, holds promise for the future of hepatoprotection and the treatment of liver diseases (Wang et al., 2021).

Materials and Methods

Materials

The whole plant of *Solanum xanthocarpum* were collected from local area of Hyderabad, Telanagana, India. Whole plant of *Solanum xanthocarpum* are authenticated by L. Rasingam, Scientist 'E' and HoO, Botanical Survey of India, Deccan Regional Center, Hyderabad. (BSI/DRC/2022-23/The. /Identification 302 and 303).

Collection and methods of extraction

Around 5kg whole plant of *Solanum xanthocarpum* were Collected, washed in running tap water and then rinsed with distilled water. Was subjected to drying at room temperature for about two weeks in open air. The dried peel were powdered using mixer grinder and passed through sieve no 22. The coarse powder was extracted with Methanol in Soxhlet's apparatus at a temperature not exceeding 40°C for 96 hours. The extract was concentrated under reduced pressure in rotary evaporator to yield a crude semi-solid mass. Then this was stored at 4 °C for further analysis

Qualitative phytochemical screening of plant extract:

1) Test for Carbohydrates:

- **Molisch test:** To the extract α-napthol and concentrated sulphuric acid was added.
- **Fehling's test:** To the extract, equal quantities of Fehling's A and B were added and heated.
- **Benedict's test:** To the extract, a few ml of benedict's reagent was added and heated.

2) Test for Alkaloids:

To the extracts dilute hydrochloric acid was added and filtered. The extract was treated with the following reagents and observed for the precipitate.

- **Mayer's reagent:** Mayer's reagent was treated with Filtrate (potassium mercuric iodide).
- **Dragendroff's reagent**: Fractions were treated with Dragendroff's reagent.
- **Hager's reagent**: Filtrate was mixed with Hager's reagent (saturated picric acid solution).

- **Wagner's reagent:** Fractions were treated with Wagner's reagent (Iodine in potassium iodide).

3) Test for Glycosides

- **Borntrager's test:** The drug was extracted with ether and the filtrate is made alkaline with caustic soda or ammonia.

4) Test for Saponins:

- To the aqueous extract, 20 ml of distilled water is added and shaken in graduated cylinder for 15 min.

5) Test for Flavonoids:

- **Shinoda test:** To the extract 5 ml of 95% ethanol and a few drops of concentrated sulphuric acid and a few magnesium turnings were added and observed for precipitate.
- **Alkaline reagent test:** To the extract add few drops of sodium hydroxide solution and observed for precipitate.

6) Test for Phenolic Compounds and Tannins:

- The extract was treated with dilute $Fecl_3$, 1% solution of gelatin containing 10% sodium chloride, 10% lead acetate and aqueous bromine solution and observed for the precipitate.

7) Test for Resins:

- The extract was treated with acetic anhydride and concentrated sulphuric acid and observed for the colour.

8) Test for Proteins and Aminoacids:

- Small quantities of alcoholic and aqueous extracts are dissolved in a few ml of water and subjected to milon's, biuret and ninhydrin tests.

9) Test for Steroids and Triterpinoids

- **Libermann-Buchard test:** To the extract add few drops of acetic anhydride, boil and cool. Then added concentrated sulphuric acid from the side of the test tube and observed for precipitate.

Gas chromatography-Mass Spectrometry (GC-MS) analysis

The Clarus 680 GC was used in the analysis employed a fused silica column, packed with Elite-5MS (5% biphenyl 95% dimethylpolysiloxane, 30 m × 0.25 mm ID × 250µm df) and the components were separated using Helium as carrier gas at a constant flow of 1 ml/min. The injector temperature was set at 260°C during the chromatographic run. The 1µL of extract sample injected into the instrument the oven temperature was as follows: 60 °C (2 min); followed by 300 °C at the rate of 10 °C min−1; and 300 °C, where it was held for 6 min. The mass detector conditions were: transfer line temperature 230 °C; ion source temperature 230 °C; and ionization mode electron impact at 70 eV, a scan time 0.2 sec and scan interval of 0.1 sec. The fragments from 40 to 600 Da. The spectrums of the components were compared with the database of spectrum of known components stored in the GC-MS NIST (2008) library.

Preparation of samples and HPTLC profiling

20 mg of *Solanum xanthocarpum* extract were dissolved individually in HPLC grade methanol and then filtered using a PTFE membrane filter of 0.2 µm pore size (Millipore, Merck, Germany). Thereafter, with the help of Camag Linomat, 6 µL of each sample were applied simultaneously with a 4 mm wide band length to pre-washed

and activated silica gel 60 F254 pre-coated HPTLC plates (20 cm × 10 cm, 200 µm thickness, Merck, Darmstadt, Germany) with the nitrogen flow providing a delivery speed of 150 nL/s. Method development was executed in a Camag twin trough glass chamber (20 cm × 10 cm) saturated with the mobile phase containing toluene/ethyl acetate/formic acid (6:3.5: 0.5, v/v/v) as a solvent system. The plate was developed horizontally to a distance of 80 mm at room temperature (25°C). After drying, the spots on the developed plates were visualized under visible light and then scanned at 254 nm and 366 nm, respectively.

Cell culture

Human hepatoblastoma cells (HepG2) were obtained from National Centre for Cell Science (NCCS) Pune, India. HepG2 cells were cultured in T-25 flasks in Dulbecco Minimal Essential Medium (DMEM-F12, Gibco) with B27 supplements, 2mM L-Glutamine and 10% fetal bovine serum (FBS) at 37°C temperature and 5% CO2 atmosphere in a CO2 incubator (Thermo scientific). HepG2 cells were sub-culture for more than 10 passages and passage 4-6 cells were used for drug toxicity studies.

IC_{50} determination of *Solanum xanthocarpum* in HepG2 cells

To identify the IC_{50} of *S. xanthocarpum* 2 X 104 HepG2 cells were cultured in each well of 96 well culture plates and allowed to grow up to 80% confluency. After reaching to confluency different concentrations of *S. xanthocarpum* (1µg/mL to 1mg/mL) were used to treat these cells each dose in triplicate for 72 hours. The concentration resulting in 50% growth inhibition was termed as IC50 of S. xanthocarpum for sensitive HepG2 cells. Control group contained only growth medium as alternative to the drug. The effect of different concentration of S. xanthocarpum in growth of HepG2 cells was evaluated at a microscopic and cellular level using 3-(4,5-dimethylthiazol-2-yl)-2,5-diphenyltetrazolium bromide (MTT) assay in triplicates, which allowed to calculate the viability of cells by colorimetry. The death rate was calculated by comparing the formazan synthesis in treated cells against the synthesis in untreated cells for each concentration after 72 hours of exposure. IC50 was calculated from the cell mortality curves.

MTT cell proliferation assay

The cytotoxic effect of the *S. xanthocarpum* in HepG2 cells was evaluated using MTT cell proliferation assay at different time points (0h to 72h). Briefly, after reaching to 80% confluency HepG2 cells were treated with 10µg/mL to 40mg/mL of *S. xanthocarpum* (diluted in culture medium) around its IC50 dose in triplicates. 40mg/mL (conc.) was used as standard drug for comparative analysis. 20µL MTT (2mg/mL) was added in each well after 0h, 4h, 8h, 12h, 24h, 48h and 72h of exposure to S. xanthocarpum in culture and incubated for additional 4 hours. After incubation, 50µL of Isopropanol was added in each well to stop the reaction and optical density was obtained using a microplate reader at 570nm (Biorad, USA). Percentage cell survival was calculated using optical density value of each sample.

Microscopy observations

Changes in cellular morphology and densities in culture plate with or without treatment with Drug 1 were documented for each group after 72 hours using Axiovert software (version 4.0) in an inverted fluorescence microscopy (Carl Zeiss, Germany).

Statistical analysis

The data were expressed in mean ± SD. Percentage cell survival was calculated by dividing optical density of HepG2 cells exposed to drug with cells without drug exposure and multiplying with 100. Similarly, IC50 value was determined using GraphPad Prism software (version V). Expression levels of each gene transcript was represented in transcript ratio and calculated using 2-ΔΔCt method.

Cell survival assay using XTT

XTT (2,3-Bis-(2-Methoxy-4-Nitro-5-Sulfophenyl)-2H-Tetrazolium-5-Carboxanilide) cell survival assay was performed in each group of cells in triplicate with or without treatment with the ECQ and ESX of lipopolysaccharide (LPS, 1µg/ml for 24 hours) exposed cells using 10uL of stock and stock diluted to 1:5, 1:10, 1:100 and 1:1000 for 2X104 HepG2 cells in each well of 96 wells plate. XTT (20µg/mL) was added after 72 hours of the culture of cells in DMEM with 10% FCS and 1X pen/strep at 37oC temperature and 5% CO2 and incubated for 4 hours and optical density was measured using a microplate reader at 570nm. Doxorubicin was used as a positive control using similar dilutions and the survival rate was compared using a line and dot plate against control.

Trypan blue assay for viability testing

The viability and count of HePG2 cells from each group were determined using Trypan Blue Exclusion Assay with the help of Cellometer Auto T4 Bright Field Cell Counter (Nexcelom). Briefly, cells were harvested through trypsinization (0.25% Trypsin-EDTA for 2 min at 37oC) and diluted 1:1 with 0.4% Trypan Blue dye, and incubated at room temperature for 5min. Further 20µL of cells with dye was loaded onto the Cellometer counting slide. The number of viable and dead cells was counted in each group and the percentage of viability and cell count was correlated with the XTT assay. Optical microscopy images were captured for cells in each group before performing the trypsinization.

FDA cell membrane integrity assay

The cell membrane integrity of HepG2 in culture with or without treatment was assessed using a Fluorescein Diacetate (FDA) fluorescence assay. Briefly, after 72 hours of treatment of HepG2 cells in 8-well chamber slides, 5µl (10µg/mL) FDA was added in each well and mounted using coverslips. Fluorescence images of cells in each group were captured using inverted fluorescence microscopy (Carl Zeiss, Germany).

Statistical analysis and software

The data in the present study has been presented as Mean ± standard deviation (SD). One-way ANOVA was used with post hoc students' t-test for comparing different groups and calculating the significant values. A p-value <0.05 was considered statistically significant. The graph was created using GraphPad Prism (version 9).

Preparation of Nano-suspension:

Precipitation method is a general method used to prepare submicron particles of poorly soluble drugs. In this method, drug is dissolved in solvent and then solution is mixed with solvent to which drug is insoluble in the presence of surfactant. Rapid addition of solution to such solvent (generally water) leads to rapid supersaturation of drug in the solution, and formation of ultrafine amorphous or crystalline drug. This method involves nuclei formation and crystal growth which are mainly dependent on temperature. High nucleation rate and low crystal growth rate are primary requirements for preparing a stable suspension with minimum particle size **[Matteucci ME, et.al.2007, Patel and Agrawal 2011]**

The nanosuspension was made using the nanoprecipitation method suggested in a previous study. Plant extract 0.25 g was dissolved in 10 mL of ethanol (organic phase) and 0.25 g of the poly vinyl alcohol stabilizer was dissolved in 100 mL of distilled water (aqueous phase). The ensuing organic layer was gradually (1 mL/min) poured with the help of a syringe into the aqueous phase with constant stirring at 1000 rpm for 6 h at room temperature. The entire formulation was stored at room temperature.

Characterization of optimized nanoemulsion:

1) Globule Size and Polydispersity Index (PDI)

Globule size is a critical parameter that may influence the composition and bioacceptability of a nano emulsion. The PDI mainly determines sample uniformity in terms of either monodisperse or polydisperse particle in a nanoemulsion. The determination of both was performed using Zetasizer Nano ZS90, Malvern Instruments, Malvern, UK) at 633 nm [25]. The different samples were analyzed in triplicate, and the results were described as mean ± standard deviation.

2) Zeta Potential

The zeta potential of an optimized nanoemulsion was measured by a dynamic light scattering technique, Zetasizer Nano (Malvern Instruments, Ltd., Malvern, UK), at room temperature and applied electric field 1 V. Prior to analysis, the formulation sample was dispersed in a prefiltered double distilled water at a ratio of 1:100. The analysis was performed in triplicate, and the result was described as mean ± standard deviation.

3) Differential Scanning Colorimetry

A differential scanning calorimeter was used for thermal analysis, which suggests the mechanism associated with the destabilization of the nanosuspension. The sample to be analyzed was crimped non hermetically in an aluminum pan and heated from 30 to 200 °C. There was an increase in temperature, which was recorded as 10 °C/min, while the nitrogen flow rate was maintained at 60 mL/min in the instrument. An amount of 5% mannitol was used as a cryoprotectant for lyophilization.

4) Transmission Electron Microscopy

To investigate the nanosuspension's morphological characteristics and to confirm the size measurement results, TEM (Zeiss, EM10C, 80 kV, Oberkochen, Germany) was

employed. A sample preparation for TEM was performed by placing one drop of 100 times diluted sample on the copper grid. Samples were stained with uranyl acetate, and a dried copper grid was placed for TEM analysis.

5) X-ray diffraction studies

The X-ray diffractograms of the prepared nanosuspension were characterized with a powdered X-ray diffractometer (model: D8 Advance; Bruker Optik GmbH, Ettlingen, Germany) using Ni-filtered radiation. Sample was deposited on the sample holder for scanning the in the range of 10°–60°.

2.2. Histopathology of rat liver (H&E staining):

After sacrificing the animals, the liver of representatives of each of the five groups that is Normal group, Induced by VPA group, VPA+STD- silymarin group, VPA+ Extract group and VPA+ Nanosuspension group.

Results and Discussion:

Percentage yield of *Solanum xanthocarpum* extract:

The coarsely powered plant materials were extracted with ethanol and successive extraction to obtain crude extracts and were further partitioned into different factions on the basis of increasing polarity are shows the colour and percentage yield in Table 1.

Table 1: Different solvent percentage yield of Solanum Xanthocarpum extract

S. No.	Extracts	Color and consistency	Percentage yield
1	Ethanolic extract	Greenish brown sticky	10.6
2	n-hexane	Dark brown	2.8
3	Chloroform	Dark brown	1.6
4	Ethyl acetate	Yellowish ash	1.9
5	n-butanol	Dark brown	3.2

Preliminary phytoconstituent analysis:

The preliminary Phytochemical studies result of extract in different solvent fractions of presence of steroid, flavonoids, glycosides, terpenoids, carbohydrates and alkaloids respectively. Phytochemical investigation of both plants' fractions is shown in Table 2.

Table 2: Preliminary phytochemical analysis of the Ethanolic, n-hexane, chloroform, Ethyl acetate and n-butanol extracts of *Solanum xanthocarpum.*

Phytochemicals	Ethanolic extract	n-hexane extract	$CHCl_3$ extract	E. acetate extract	n-butanol extract
Alkaloids	-	-	-	-	-
Carbohydrates	+	-	-	-	+
Flavonoids	+	-	+	+	-
Glycosides	+	-	+	+	-

Proteins	+	-	-	-	+
Steroids	+	+	-	-	-
Saponins	+	+	+	+	-
Tannins	+	-	-	+	-
Terpenoids	+	+	+	+	-

Investigation of the components of n-hexane extract of *Solanum xanthocarpum* using GC-MS analysis

The result of the GC-MS analysis of n-hexane extract of *Solanum xanthocarpum* leaves is shown in Figure 1 and Table 3. It revealed the presence of 34 compounds were identified. Those of reference compounds analysed under the same conditions.

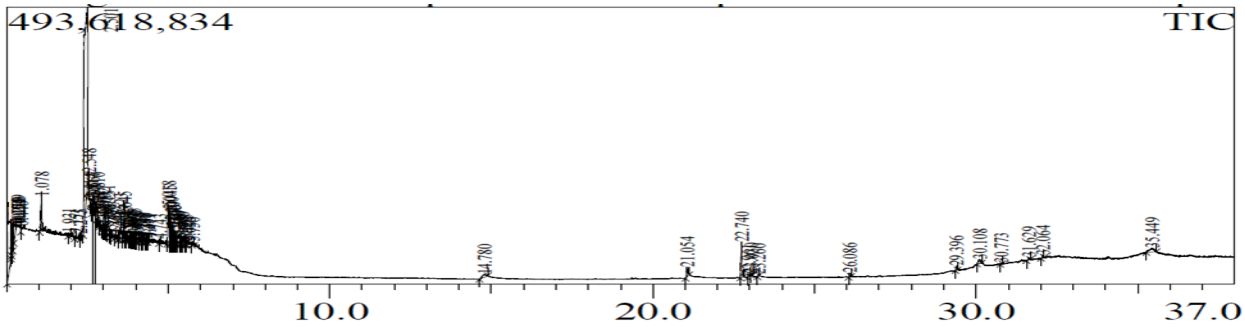

Figure 1: GC-MS chromatogram of n-hexane extract of *Solanum xanthocarpum* plant.

Table 3: Identification of the components of n-hexane extract of *Solanum xanthocarpum* plant.

S. No	Peak Name	Molecular Structure	Molecular Formula	Molecular Weight	Retention Time	% Area
1	2-Nonynoic acid	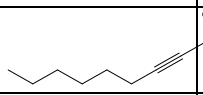	$C_9H_{14}O_2$	154	0.129	9.72
2	Acetic acid, difluoro-, methyl ester	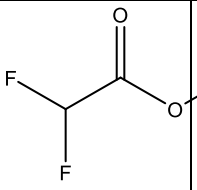	$C_3H_4F_2O_2$	110	0.150	0.80
3	N,N'-Ethylenebis(N-nitroacetamide)	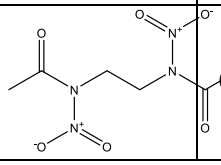	$C_6H_{10}N_4O_6$	234	0.446	0.11

4	(S)-(-)-2-Chloropropionic acid	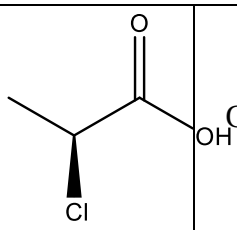	$C_3H_5ClO_2$	108	1.078	1.27
5	Ethane, 1-chloro-1-fluoro-	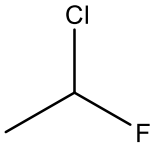	C_2H_4ClF	82	1.931	0.19
6	2-Propanone, 1-hydroxy-	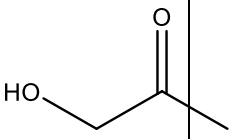	$C_3H_6O_2$	74	2.151	0.28
7	2-Propanone, 1,1-dichloro-	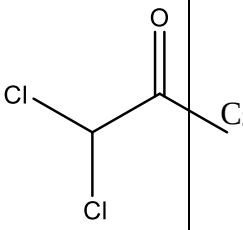	$C_3H_4Cl_2O$	126	2.275	0.16
8	Ethene, 1-(2-methoxy-,3,5-dibromophenyl)-2-nitro-	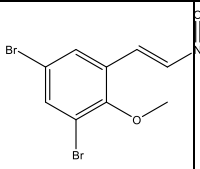	$C_9H_7Br_2NO_3$	104	2.501	38.64
9	Cyclohexane, 1,4-dimethyl-, cis	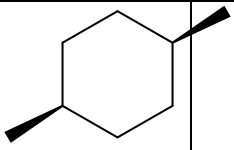	C_8H_{16}	112.2	2.548	0.30
10	3-Hexene-2,5-dione	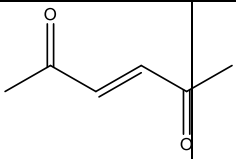	$C_6H_8O_2$	112	2.614	0.26
11	Cyclopentane, 1-hexyl-3-methyl-	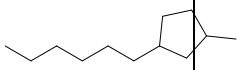	$C_{12}H_{24}$	168	2.667	0.39
12	Cyclohexane, 1,3-dimethyl-, trans-	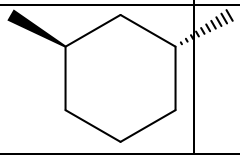	C_8H_{16}	112	2.810	0.84

13	1,5-Diacetoxypentane	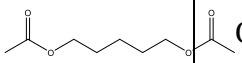	$C_9H_{16}O_4$	188	2.878	0.36
14	Cycloheptene, methyl-	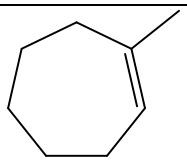	C_8H_{14}	110	2.949	0.18
15	4-Decene, 7-methyl-, (E)-	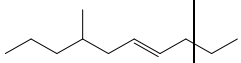	$C_{11}H_{22}$	154	3.002	0.65
16	4-Octyne, 2-methyl-	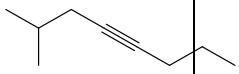	C_9H_{16}	124	3.051	0.49
17	2-Hexanone, 3-methyl-4-methylene-	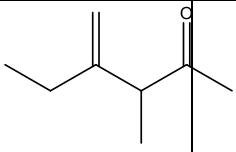	$C_8H_{14}O$	126	3.523	1.33
18	1,6-Heptadien-3-yne, 5-methyl-	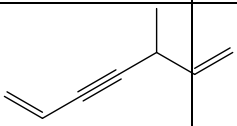	C_8H_{10}	106	3.645	1.78
19	Cyclopentene, 1-ethenyl-3-methylene-	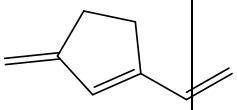	C_8H_{10}	106	4.411	0.13
20	2H-Pyran-2,6(3H)-dione, dihydro-	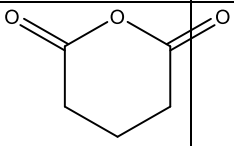	$C_5H_6O_3$	114	5.018	3.09
21	1,4-Cyclohexadiene-1,2-dicarboxylic anhydride	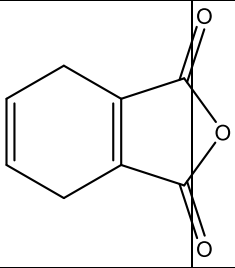	$C_8H_6O_3$	150	5.018	3.09
22	1,7-Octadiyne	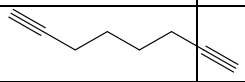	C_8H_{10}	110	5.355	0.24
23	N,N-Dinitro-1,3,5,7-tetrazabicyclo[3,3,1]nonane-	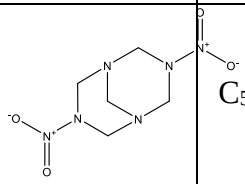	$C_5H_{10}N_6O_4$	218	5.625	0.27
24	(1R,3R,4R,5R)-(-)-Quinic acid	-	$C_7H_{12}O_7$	192	14.780	0.59

25	n-Hexadecanoic acid	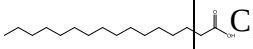	$C_{16}H_{32}O_2$	256	21.054	0.75
26	Hexadecanal	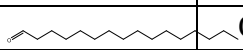	$C_{16}H_{32}O$	240	22.740	1.80
27	Cyclodecene, (Z)-	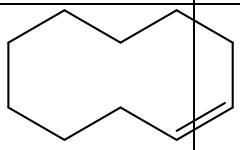	$C_{10}H_{18}$	138	22.961	0.07
28	9,12,15-Octadecatrienal	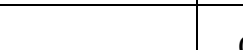	$C_{18}H_{30}O$	262	23.030	0.06
29	(E,E,E)-3,7,11,15-Tetramethylhexadeca-1,3,6,10,14-pentaene	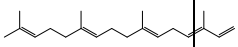	$C_{20}H_{32}$	272	26.086	0.20
30	Decanoic acid, decyl ester	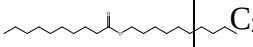	$C_{20}H_{40}O_2$	312	30.108	0.56
31	Vitamin E	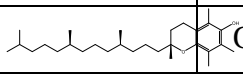	$C_{29}H_{50}O_2$	430	30.773	0.04
32	Ethyl iso-allocholate	-	$C_{24}H_{45}O_5$	436	31.629	0.15
33	trans-Z-alpha.-Bisabolene epoxide	-	$C_{15}H_{24}O$	220	32.064	0.13
34	2-Tridecenal, (E)-	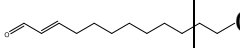	$C_{13}H_{24}O$	196	35.449	1.00

HPTLC Fingerprinting:

Herbal products contain several verities of secondary metabolites with large chemical diversity, and it is very difficult to target a particular constituent concerning their biological activity. In these cases, TLC fingerprint profiling of herbal products is very useful and widely used for qualitative and quantitative evaluation. The compounds separated on the TLC plate at different Rf values represent the number of chemical constituents present in the mixture/extract. Moreover, in HPTLC finger printing of *Solanum xanthocarpum*, the plate was developed in the defined solvent system n-butanol: water: glacial acetic acid (6:3:1, v/v/v) and scanned at 254 and 366 nm. HPTLC chromatographic analysis of different batches of samples showed 7 and 5 prominent spots at different values at 254, and 366 nm, respectively. The chromatographic profiling revealed that

several major and minor constituents present in the methanolic extract of *Solanum xanthocarpum*. The constituent intensity was identified according to their AUC value/peak intensity (Figure 2).

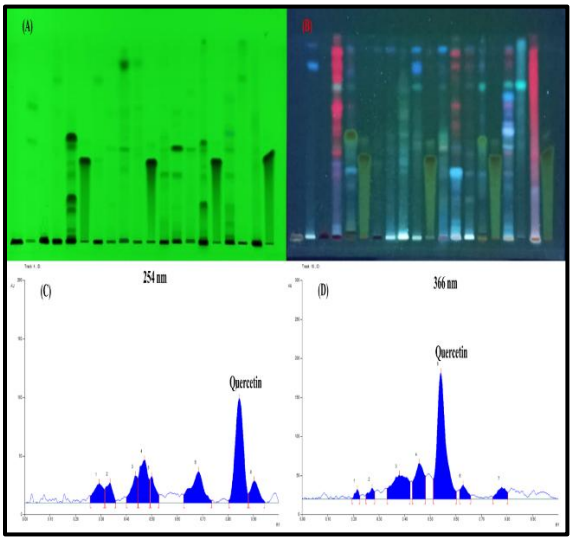

Figure 2: HPTLC plate view at 254 nm and 366 nm and different chromatograms of *Solanum xanthocarpum* at different wavelengths. (A) represents view at 254 nm are the standard of Quercetin track of different batches of *Solanum xanthocarpum*, (B) represents view at 366 are the standard of Quercetin of different batches of *Solanum xanthocarpum*. (C) show chromatograms of the sample at 254, respectively, whereas (D) shows chromatogram of mixed standard at 366 nm.

Morphometric assessment of HepG2 cells:

The qualitative morphometric assessment after treatment with ESX at different dilutions showed improved cell morphology of surviving HepG2 cells than untreated cells (Figure 2). Both the numbers and intercellular connections were improved after ESX treatment. The highest improvement in cell morphology and numbers was observed for 1:10 dilution of ESX-treated cells.

IC50

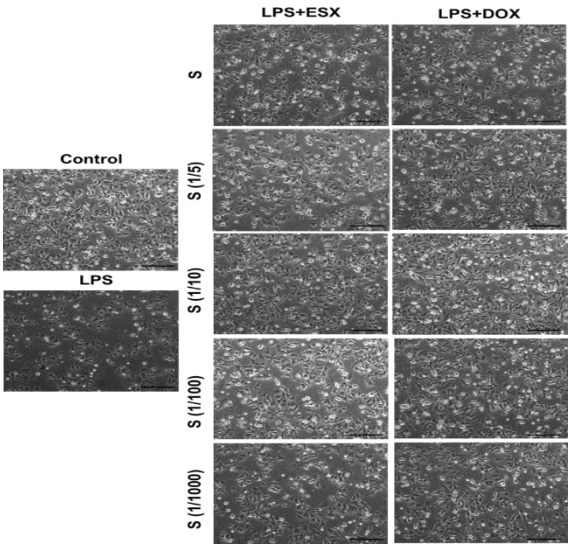

Figure 3: Bright field microscopic images showing morphological changes and variable numbers of viable HepG2 cells with or without ESX treatment after 72 hours. Magnification 20X, Scale bar: 100µm.

Comparative cell membrane integrity of HepG2 cells:

Similar to the bright field microscopy observations, the cell membrane integrity assay through FDA staining showed improved cell membrane integrity after treatment with ESX at different dilutions than untreated cells which is evident by the increased green fluorescence in HepG2 cell membranes (Figure 3).

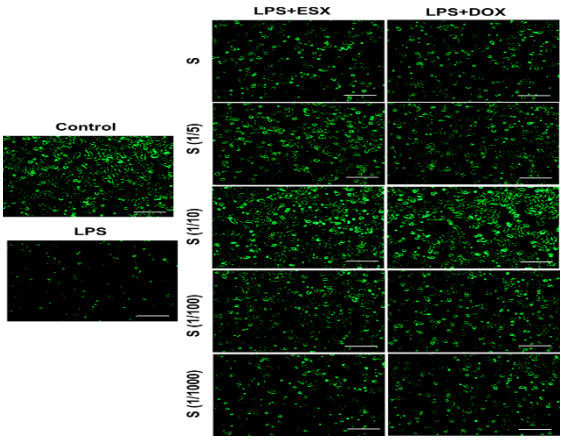

Figure 4: Fluorescence inverted microscopy images showing green fluorescence in cells having intact membranes. Magnification 20X, Scale bar: 100µm.

Cell viability and counts of HepG2:

Cell viability assessment through trypan blue exclusion assay of HepG2 cells after treatment with ESX at different dilutions showed improved survival than untreated cells (Figure 4A). This observation was further validated by counting viable cells in each group (Figure 4B). Cell counting results showed a significantly increased number of viable HepG2 cells after treatment with undiluted ESX (2882±88 vs ±2368±193, p=0.002) followed by 1:10 dilution (3267±173 vs 2415±93, p=0.004), 1:5 (2975±93 vs 2392±88, p=0.02), and 1:100 dilutions (2940±70 vs 2368±193, p=0.02), while no significant difference was observed for 1:1000 dilution (p>0.05) when compared to the untreated group (LPS).

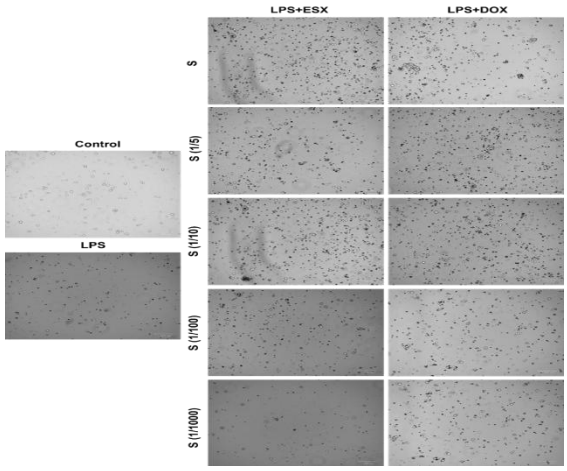

Figure 5A: Microscopic trypan blue images showing live and dead HepG2 cells with or without ESX treatment after 72 hours. Dead cells are stained in blue while live cells exclude trypan blue and appear bright. Magnification 20X, Scale bar: 100µm.

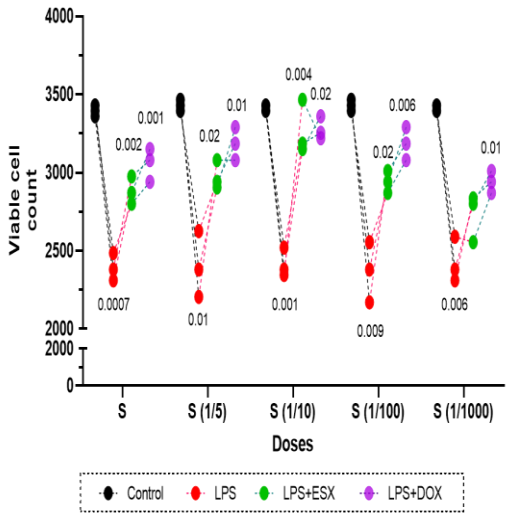

Figure 4B: Dot and line plot showing a significant increase in the number of viable HepG2 cells after 72 hours of exposure to ESX in a dose-dependent manner. Each dot represents the value of cells that survived in a single well in a cohort of trypan blue exclusion assay performed in triplicate. The values indicated above or below each dot point

represent a p-value of that particular data set compared between control and LPS, and LPS and LPS-treated cells with different dilutions of ESX.

IC50: Please provide us result

Validation of cell survival using XTT assay:

The in vitro XTT assay of ESX in LPS-treated cells showed the highest proportion of HepG2 cell survival at 1:10 dilution (91.33% vs 69.33%, p=0.002) followed by 1:5 (85.33% vs 69.33%, 0.008), 1:100 (83.00% vs 69.33%, p=0.01), and undiluted ESX (82.66% vs 69.33%, p=0.01) compared to untreated cells (LPS group). We didn't observe significant improvement in HepG2 cell survival at 1:1000 dilution of ESX (76.66% vs 69.33%, p>0.05, Figure 5). The LPS-treated cells showed approximately 65% cell survival compared to untreated cells (control condition, 98.33% vs 69.33%, p=0.0007). While no significant difference was observed between the control and ESX-treated groups (except 1:1000 dilution) and were almost comparable to the positive control group (LPS+DOX, p>0.05).

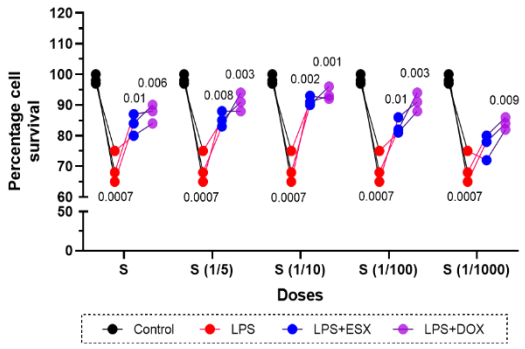

Figure 6: Dot and line plot showing a significant increase in the proportion of HepG2 cell survival after 72 hours of exposure to ESX in a dose-dependent manner. Each dot represents the value of cells that survived in a single well in a cohort of XTT assay performed in triplicate. The values indicated above or below each dot point represent a p-value of that particular data set compared to LPS-treated cells.

Histopathology of rat liver (H&E staining):

Control group: Histological section showed normal hepatic lobules with centrally located central vein and peripherally located portal triad with prominent round nuclei and eosinophilic cytoplasm arranged in plates with separate hepatic sinusoids. The portal triad of the hepatic artery, portal vein, and bile duct in normal characteristic features (Fig. A).

VPA induced group: The liver of VPA-intoxicated rats showed massive fatty change and centrilobular necrosis with mononuclear cells infiltration around central veins and in portal areas were observed (Fig. B).

STD- silymarin group: The standard silymarin-treated rats showed regular tissue architecture (Fig. C).

Extract group: Extract treated rats presented reduction in cellular hypertrophy, sinusoidal space and inflammatory cell infiltration around the central and portal areas with regeneration of hepatocytes (Fig. D).

Nanosuspension: The liver of Nano 2 treated exhibited clear hepatic tissue regeneration exhibiting normal characteristic features comparable to control group (Fig. E).

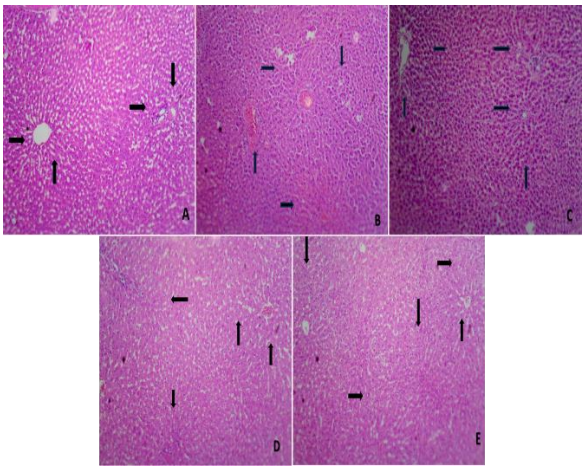

Figure 7: The histopathological section evaluation of the liver displayed (Fig A) normal hepatic lobules with centrally located central vein and peripherally located portal, (Fig B) massive fatty change and centrilobular necrosis with mononuclear cells infiltration around central veins and in portal areas, (Fig C) regular tissue architecture, (Fig D) reduction in cellular hypertrophy, sinusoidal space and inflammatory cell infiltration around the central and portal, (Fig E) treated exhibited clear hepatic tissue regeneration.

Particle size, polydispersity index (PDI), and zeta potential:

The optimized drug-loaded nanoformulation demonstrated a particle size of 262.2 ± 68.5 nm, a polydispersity index (PDI) of 0.481 ± 0.018, and a zeta potential of −18.4 ± 0.11 mV. The nanoscale dimensions enhance surface area, thereby improving drug delivery, absorption, and retention. Nanoemulsions generally exhibit particle sizes between 5 and 300 nm, with the current formulation falling within this range. The low PDI value suggests a monodisperse particle size distribution, indicating uniformity. This result implies a high surfactant concentration, which forms a dense layer at the oil–water interface, contributing to the stability and emulsification of the oil phase without relying heavily on a co-surfactant. The negative zeta potential is likely due to the presence of non-ionic surfactants, which help stabilize the emulsion and minimize the charge on the dispersed oil droplets.

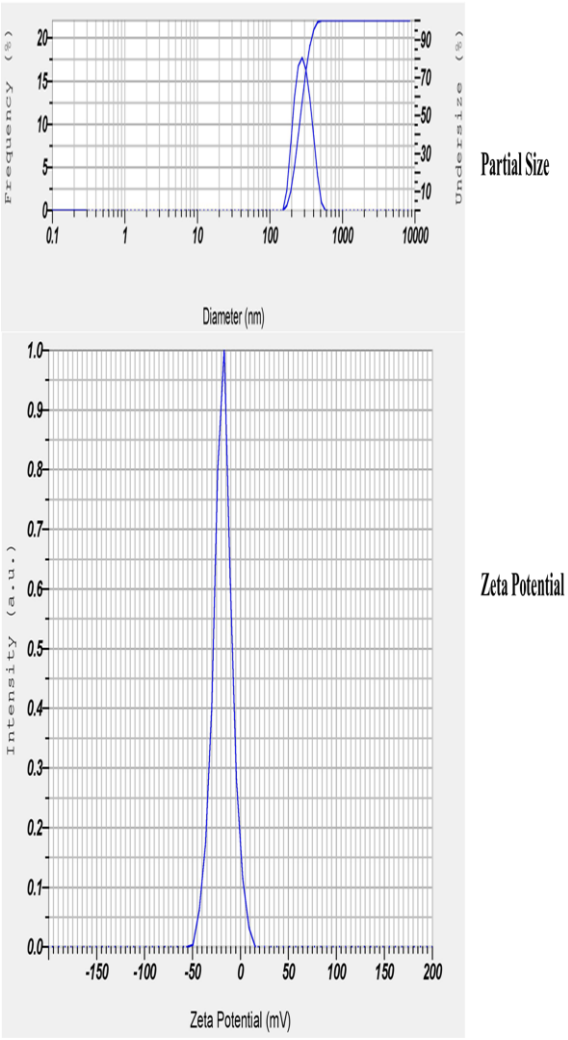

Figure 8: Particle size, polydispersity index (PDI), and zeta potential of drug loaded Nanoemulsion.

Differential scanning calorimetry (DSC):

The melting point of the EXT-ESX tad drug was determined to be 42.74 °C (Figure 8), which aligns with the reported melting range of 30 to 70 °C. The

obtained thermal event was exothermic, indicating the crystalline nature of the drug. Differential scanning calorimetry (DSC) analysis of the Nano Suspension ESX tad showed a peak at 45.07 °C, whereas the Nano Suspension CQ tad combination exhibited a peak at **00.00 °C**. In the DSC thermogram of the optimized Nano Suspension ESX tad combination formulation, only a single peak at 00.00 °C was observed. This peak was closest to that of the cryoprotectants B, C, and D, which were added prior to the lyophilization of the optimized nanosuspension. The presence of a single peak might be attributed to the high content of EXT-ESX tad, suggesting a transition of both EXT-ESX tad and Nano Suspension ESX tad from a crystalline to an amorphous state, without any significant peak observed. This transition could enhance the stability of the formulation by preventing leaching or precipitation of EXT-ESX tad and Nano Suspension ESX tad.

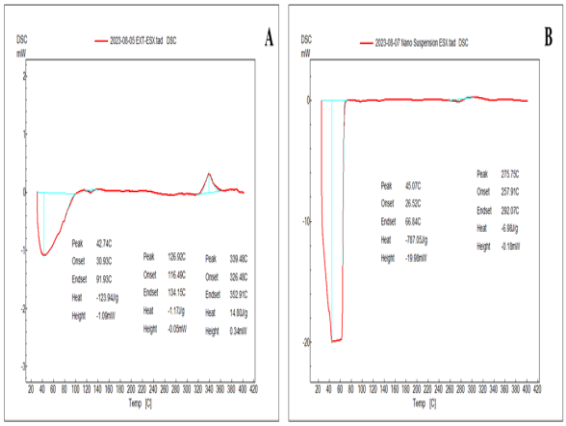

Figure 9: Overlay of Differential scanning calorimetry (DSC) A (EXT-ESX tad), B (Nanosuspension ESX).

X-Ray Diffraction:

The X-ray diffraction (XRD) patterns, presented in Figure 9, illustrate the crystalline characteristics of the pure drug, ESX raw, indicated by sharp peaks at 2θ values of 25° and 45°. In contrast, the Nano ESX raw exhibited reduced crystallinity, with small amorphous peaks observed at 2θ values of 20° and 35°. The lyophilized formulation displayed a transformation from a crystalline to an amorphous state, lacking significant peaks. However, a few distinct peaks were still observed at 2θ values of 25° and 42°. The reduction in peak intensity suggests an amorphous nature of the formulation. This conclusion is further corroborated by the differential scanning calorimetry (DSC) analysis, as previously discussed in this section.

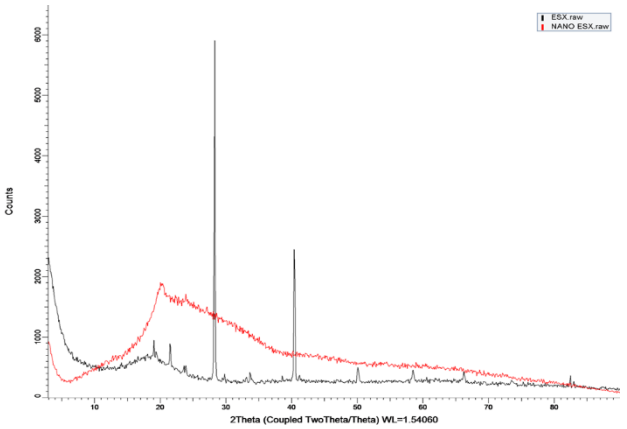

Figure 10: Overlay of X-ray diffractograms of ESX raw and Nano ESX raw. Major peaks of ESX raw were almost disappeared in the nanoemulsion, suggesting that the crystallinity of the ESX raw has lost after the solubilization by nano ESX raw.

Transmission Electron Microscopy (TEM) and Scanning Electron Microscopy (SEM):

Two distinct techniques were utilized to examine the structure and surface morphology of the final formulation. These methods collectively indicated a spherical, globule-like morphology with a size below 500 nm (Figure 10). Moreover, the observed size distribution was consistent with the measurements obtained using a zeta sizer. Therefore, the optimized formulation meets the desired criteria for shape and size-specifically, nanometric and globular-suggesting its

suitability for effective topical delivery, permeation, and retention.

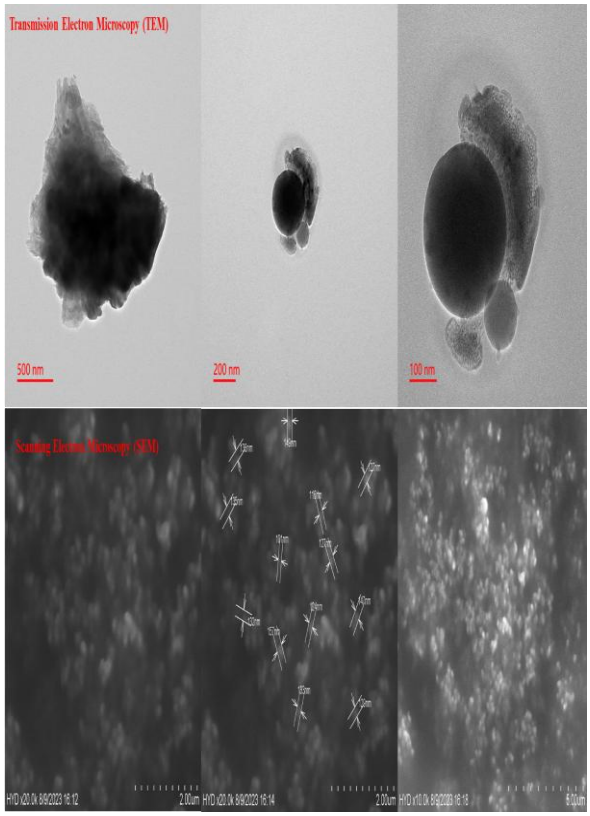

Figure 11: Transmission Electron Microscopy (TEM) and Scanning Electron Microscopy (SEM) of optimized Nano ESX nanoformulation.

Conclusion:

The study highlights the hepatoprotective potential of *Solanum xanthocarpum*, specifically in the form of nanosuspensions, as a promising therapeutic approach for liver diseases. The utilization of *Solanum xanthocarpum* in traditional medicine, particularly in Ayurveda, is rooted in its diverse pharmacological activities, including antioxidant, anti-inflammatory, and hepatoprotective effects. By leveraging nanotechnology, nanosuspensions of *Solanum xanthocarpum* extracts were formulated to enhance the bioavailability and efficacy of these bioactive compounds, achieving improved solubility, stability, and therapeutic outcomes. The nanoscale particle size allowed for a larger surface area, contributing to enhanced drug dissolution, absorption, and retention, ultimately increasing the therapeutic efficacy.

The study utilized various assays, including IC50 determination, MTT cell proliferation, XTT cell survival, and membrane integrity assessments, which demonstrated the improved viability and morphological characteristics of HepG2 cells treated with *Solanum xanthocarpum* nanosuspensions. The enhanced delivery of active compounds to the liver is attributed to the nanosuspension formulation, which also provided sustained release and reduced the frequency of dosing—an essential feature for long-term management of chronic liver diseases. Overall, *Solanum xanthocarpum* nanosuspensions exhibited significant potential in mitigating liver injury through their antioxidant, anti-inflammatory, and hepatoprotective properties. The findings underscore the promising role of herbal nanomedicine in modern therapeutics, providing a safer, more effective, and holistic approach for the treatment of liver diseases such as NAFLD, hepatitis, and liver fibrosis. This advancement in hepatoprotective strategies reflects a growing recognition of natural compounds enhanced by nanotechnology, presenting a novel avenue for liver disease treatment with fewer side effects compared to conventional synthetic drugs. Future research should focus on clinical trials to further explore and validate the efficacy and safety.

References:

- *Ahmad, M.F., Ahmad, F.A., Zeyaullah, M., Alsayegh, A.A., Mahmood, S.E., AlShahrani, A.M., Khan, M.S., Shama, E., Hamouda, A., Elbendary, E.Y., Attia, K.A.H.A., 2023. Ganoderma lucidum: Novel Insight into Hepatoprotective Potential with Mechanisms of Action. Nutrients.*

https://doi.org/10.3390/nu15081874

- *Arman, M., Chowdhury, K.A.A., Bari, M.S., Khan, M.F., Huq, M.M.A., Haque, M.A., Capasso, R., 2022. Hepatoprotective potential of selected medicinally important herbs: evidence from ethnomedicinal, toxicological and pharmacological evaluations. Phytochemistry Reviews. https://doi.org/10.1007/s11101-022-09812-5*
- *Ayenew, K.D., Wasihun, Y., 2023. Hepatoprotective effect of methanol extract of Agave americana leaves on paracetamol induced hepatotoxicity in Wistar albino rats. BMC Complementary Medicine and Therapies. https://doi.org/10.1186/s12906-023-03931-y*
- *Coronati, M., Baratta, F., Pastori, D., Ferro, D., Angelico, F., Del Ben, M., 2022. Added Fructose in Non-Alcoholic Fatty Liver Disease and in Metabolic Syndrome: A Narrative Review. Nutrients 14, 1127. https://doi.org/10.3390/nu14061127*
- *Gautam, G., Parveen, R., Ahmad, S., 2023. LC-MS-based Metabolomics of Medicinal Plants, in: Omics Studies of Medicinal Plants. https://doi.org/10.1201/9781003179139-9*
- *Haqqi, A., Munir, R., Khalid, M., Khurram, M., Zaid, M., Ali, M., Shah, Z.H., Ahmed, H., Afzal, M.S., 2019. Prevalence of Hepatitis C Virus Genotypes in Pakistan: Current Scenario and Review of Literature. Viral Immunology 32, 402–413. https://doi.org/10.1089/vim.2019.0058*
- *Harakeh, S., Saber, S.H., Al-Raddadi, R., Alamri, T., Al-Jaouni, S., Qari, M., Qari, Y., Haque, S., Zawawi, A., Ali, S.S., Elmageed, Z.Y.A., Mousa, S., 2023. Novel curcumin nanoformulation induces apoptosis, and reduces migration and angiogenesis in liver cancer cells. Artificial Cells, Nanomedicine and Biotechnology. https://doi.org/10.1080/21691401.2023.2238756*
- *Hussain, T., Gupta, R.K., Sweety, K., Eswaran, B., Vijayakumar, M., Rao, C.V., 2012. Nephroprotective activity of Solanum xanthocarpum fruit extract against gentamicin-induced nephrotoxicity and renal dysfunction in experimental rodents. Asian Pacific Journal of Tropical Medicine. https://doi.org/10.1016/S1995-7645(12)60107-2*
- *Jain, D., Chaudhary, P., Kotnala, A., Hossain, R., Bisht, K., Hossain, M.N., 2020. Hepatoprotective activity of medicinal plants: A mini review. Journal of Medicinal Plants Studies 8, 183–188. https://doi.org/10.22271/plants.2020.v8.i5c.1212*
- *Kim, W., 2022. Hepatocellular Carcinoma, in: Sex/Gender-Specific Medicine in the Gastrointestinal Diseases. https://doi.org/10.1007/978-981-19-0120-1_15*
- *Konar, A., Chatterjee, R., 2022. Solanum Xanthocarpum-A Critical Approach to the Lesser Known Aspects of the Herb. International Journal of Scientific Research in Biological Sciences.*
- *Kulik, L., El-Serag, H.B., 2019. Epidemiology and Management of Hepatocellular Carcinoma. Gastroenterology. https://doi.org/10.1053/j.gastro.2018.08.065*
- *Kumar, P., Shakya, R., Kumar, V., Kumar, D., Chauhan, R.P.S., Singh, H., 2023. Chemical constituents and strong larvicidal activity of Solanum xanthocarpum among selected plants extracts against the malaria, filaria, and dengue vectors. Journal of Vector Borne Diseases. https://doi.org/10.4103/0972-9062.361177*
- *Kumar, S., Pandey, A.K., 2022. Pharmacological potential of serially extracted Solanum xanthocarpum fruit extracts and their phytochemical characterization. Journal of Herbs, Spices & Medicinal Plants 28, 427–441. https://doi.org/10.1080/10496475.2022.2079793*